Precision Measurement of the Mass Difference $m_{\pi^-} - m_{\pi^0}$

J. F. Crawford, M. Daum, R. Frosch, B. Jost, and P.-R. Kettle

Schweizerisches Institut für Nuklearforschung, CH-5234 Villigen, Switzerland

and

R. M. Marshall and K. O. H. Ziock

Physics Department, University of Virginia, Charlottesville, Virginia 22901

(Received 9 December 1985)

Using the time-of-flight method to determine the velocity of the neutrons from the reaction $\pi^- + p \rightarrow \pi^0 + n$ at rest we have measured the mass difference $m_{\pi^-} - m_{\pi^0}$ to be 4.5930 ± 0.0013 MeV/c^2. From the width of the time-of-flight distributions we conclude that the pionic hydrogen atoms have a mean kinetic energy $\bar{T}_{\pi p} < 12$ eV (90% confidence limit) at the time of the charge exchange.

In the last two decades the uncertainty in the mass of the charged pion has been reduced by a factor of about 20 while no improved measurements of the mass difference $D_\pi = m_{\pi^-} - m_{\pi^0}$ have been made. As a consequence the uncertainty of the 1984 world average of m_{π^-}, $\sigma(m_{\pi^-}) = 0.7$ keV/c^2, is considerably smaller than $\sigma(m_{\pi^0}) \approx \sigma(D_\pi) = 3.7$ keV/c^2.[1] While this alone provides a strong motive to reduce the error in D_π, there is a more specific reason: The pion β-decay rate can be calculated in the standard weak-interaction model. A new measurement of this quantity has been performed,[2] and another one, planned at the Schweizerisches Institut für Nuklearforschung (SIN),[3] should reduce the error of the decay rate to less than 1%. The phase space available for this decay rises as the fifth power of D_π. An optimal comparison with theory thus requires an uncertainty of $\sigma(D_\pi)/D_\pi < 0.001$; this condition is not safely met by the current world average.

In the charge-exchange reaction

$$\pi^- + p \rightarrow \pi^0 + n, \tag{1}$$
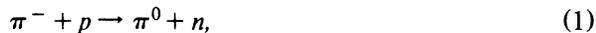
the mass difference D_π is related to the kinetic energy T_n of the neutron through energy and momentum conservation. The kinetic energy T_n can be determined by measurement of the time of flight (TOF) of the neutrons over a known distance. This technique was used in several earlier determinations of D_π.[4-7] In these experiments the neutron time of flight was measured by comparison of it with the travel time of a reference signal in a delay cable. As the main improvement in the present experiment, the measurement of signal velocities in delay cables could be avoided thanks to the use of the SIN cyclotron radio-frequency beam structure, to be described below. In addition, the statistical uncertainty has been greatly reduced.

The experimental setup is shown in Fig. 1. A beam of negatively charged pions from the SIN pion channel $\pi E1$ was stopped, after moderation in a graphite degrader, in a cylindrical liquid hydrogen (LH$_2$) target of 9-cm diam and 1.6-cm width. At the chosen beam momentum of 220 MeV/c electrons in the beam were separated in time from the pions by 11 ns at the end of the beam line. This made it possible to suppress the substantial electron background by the requirement of
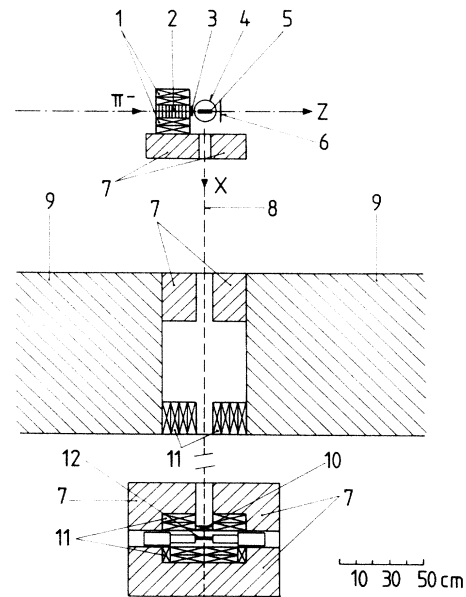

FIG. 1. Schematic of the experimental setup: (1) lead collimator; (2) graphite degrader; (3) S1 scintillation counter; (4) vacuum envelope of the target; (5) liquid hydrogen target; (6) S2 scintillation counter; (7) CH$_2$ shielding; (8) central neutron trajectory; (9) concrete shielding; (10) lead convertor; (11) lead shielding; (12) S3 scintillation counter.
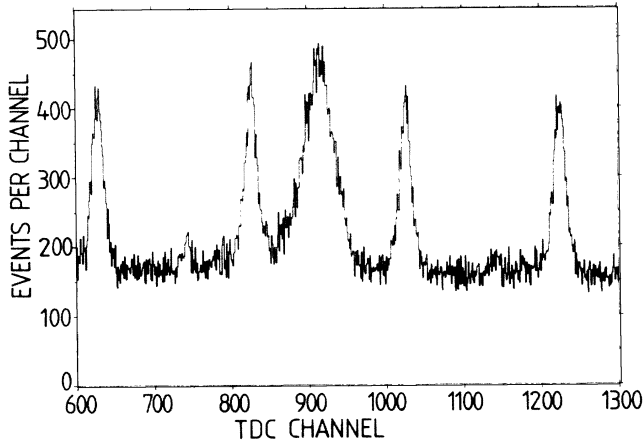

FIG. 2. Time-of-flight spectrum measured at a distance of $d_1 = 2.819$ m between the liquid hydrogen target and the neutron detector. The peak around channel 910 is due to neutrons from reaction (1). The narrow peaks stem from photons from reactions (1) and (2) interacting in the lead converter (item 10, in Fig. 1). Time increases to the left.

FIG. 3. Same as Fig. 2 but measured at a distance $d_2 = 8.440$ m from the hydrogen target.

a coincidence between the signal from the scintillator S1 (item 3, Fig. 1) and the radio frequency, rf, from the accelerator. The pions entered the target through the cylinder mantle and the neutrons were observed along the direction of the cylinder axis. The target was placed between the scintillation counters S1 and S2. A coincidence $(S1 \cdot rf) \cdot \overline{(S2 \cdot rf)}$ indicated a stopping pion. Neutrons from reaction (1), after passing a system of CH_2 and lead collimators, were identified with scintillation counter S3 (NE102A). The scintillator S3 was surrounded by an inner lead shield and an outer shield of paraffin; S3 was shielded by collimators (items 7, 9, and 11 in Fig. 1) against radiation from sources other than the LH_2 target. The scintillation counter S3 had a thickness of 1.6 cm. It presented an area of 7×9 cm^2 to the target and was viewed from the sides through "fishtail" light guides by two photomultiplier tubes (Philips XP 2230 B).

Time-of-flight spectra were taken at two distances LH_2-S3, namely at 2.819 m, then at 8.440 m, and finally at 2.819 m again; the summed spectra are shown in Figs. 2 and 3. The peak around channel 910 in Fig. 2 (1090 in Fig. 3) is attributed to neutrons from reaction (1). This interpretation was confirmed by our moving the neutron detector a few centimeters, which resulted in the expected shift of the time-of-flight peak. The peaks around channels 630, 830, 1030, and 1230 (780, 980, 1180, and 1380 in Fig. 3) stem from π^0 decays into two gammas and from the radiative capture process

$$\pi^- + p \rightarrow \gamma + n. \tag{2}$$

Some of these gammas produce $e^+ e^-$ pairs in a lead

converter placed immediately in front of S3 (cf. Fig. 1) and serve as a precise time calibration as a result of the stable radio frequency of the cyclotron; the spacing in time of these gamma peaks is $19.750\,03 \pm 0.000\,01$ ns. The small peaks around channels 740 and 1140 (890 and 1290 in Fig. 3) are attributed to bremsstrahlung from beam electrons 11 ns before each pion burst and are also present underneath the neutron peaks. For the determination of the shape of the neutron peak the background can be eliminated through pulse-height discrimination, as can be seen from Fig. 4, and the periodicity (19.75 ns) of the accidental background
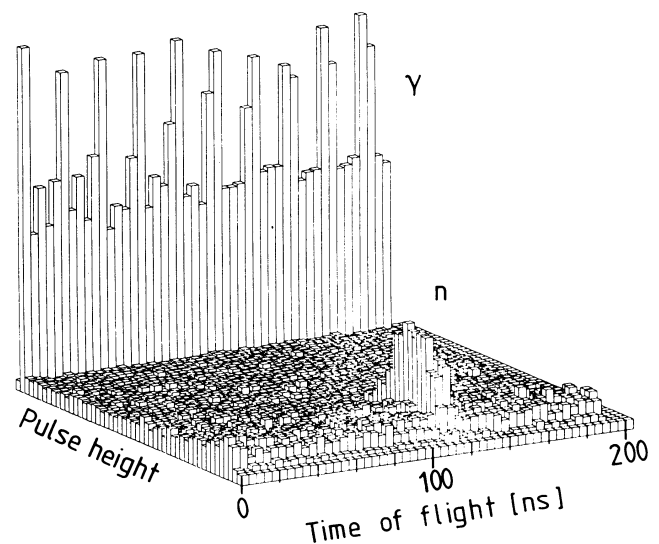

FIG. 4. Two-dimensional histogram of the time of flight and pulse height in the neutron detector. Neutrons from reaction (1) are seen around 120 ns. Gammas lead to high-energy deposition in S3 and are seen in the overflow channel with a period of 19.75 ns.

spectrum. The use of the accidental gamma peaks shown in Figs. 2 and 3, together with the fact that only standard logic signals were propagated through the delay cables, allows us to avoid the difficult investigations of signal propagation in long delay cables, needed in earlier experiments.

In our analysis, the neutron velocity is determined essentially from the location of the neutron peak relative to the adjacent gamma peaks:

$$v_n = \{[\tau_{n_2} - \tau_{n_1} + (n_2 - n_1)\tau_0]/(d_2 - d_1) + 1/c\}^{-1}. \tag{3}$$

Here the index $i = 1$, 2 refers to the two positions $d_1 = 2.819$ m and $d_2 = 8.440$ m at which we measured the time of flight; τ_{n_i} is the time from the neutron peak to the preceding gamma peak, $\tau_0 = 19.75003$ ns is the interval between the gamma peaks, and c is the velocity of light. It should be noted that only the precisely measured difference $d_2 - d_1 = 5.621$ m enters into Eq. (3) and not the less well known absolute distances between the LH_2 target and S3.

Our method relies on the knowledge of the number of rf periods that have elapsed between the stopping of a pion, $(S1 \cdot rf) \cdot \overline{(S2 \cdot rf)}$, and the beginning of the rf period in which the neutron peak is located at d_1 and d_2, respectively. We have derived n_1 and n_2 from the current world average[1] of D_π and found them to be $n_1 = 15$ and $n_2 = 46$. These numbers agree with those derived from the length of the delay cables used in our experimental setup.

In the final data analysis the neutron velocity v_n was derived by use of a Monte Carlo computer program to fit the position and the shape of the neutron TOF peaks. The inputs for this program were (1) the spatial distribution of the stopping pions in the LH_2 target, which was determined to be homogeneous in the neutron-flight-path direction; (2) the size and position of the neutron detector; and (3) the sizes and positions of the collimators. The program treats neutron energy loss through scattering in the LH_2 target, the collimator jaws, the air molecules on the flight path, the lead converter, the neutron detector, and the shielding of the neutron detector (cf. Fig. 1). The distribution of transit times from the neutron signal in the detector to the start of the conversion in the time-to-digital converter was determined by unfolding of the distribution, measured during data taking, of the time difference between corresponding signals from the two photomultipliers viewing the neutron detector. The fact that this time distribution is different for signals generated by neutrons and gammas does not affect the validity of Eq. (3), since the differences are the same for both neutron flight paths d_i.

The Monte Carlo TOF distributions for the two flight-path lengths d_i are fitted with six free parameters

to the experimental distributions of Figs. 2 and 3, after background subtraction, with use of the standard program MINUIT.[8] The free parameters are (1) the neutron velocity v_n; (2) the distance from target to detector at the data-taking point called "$d_1 = 2.819$ m" (the difference $d_2 - d_1$ was a fixed parameter); (3) the standard deviation σ_c of the distance-independent time spread, found to be consistent with a Gaussian, due to the spread of the differences between the time of reaction (1) and that of the corresponding radio-frequency signal; (4) the standard deviation $\sigma_d d$ of the distance-dependent time spread due to the motion of the $\pi^- p$ atom, to be discussed below; (5) the normalization factor for the ordinate (events per TOF bin) at $d_1 = 2.819$ m; and (6) the normalization factor for the ordinate at $d_2 = 8.440$ m. Thus the fitted variables of points (1) and (4) above are the physics results of the analysis.

The χ^2 of the fit was 300 for 250 degrees of freedom (d.o.f.). The fact that χ^2/d.o.f. is greater than 1 is attributed to the assumption of a Gaussian distribution for point (4) above. The MINUIT uncertainties[8] were multiplied by a "scale factor"[4] of $(\chi^2/\text{d.o.f.})^{1/2}$.

The result for the neutron velocity v_n is

$$v_n = 0.89418 \pm 0.00017 \text{ cm/ns}. \tag{4}$$

The quoted uncertainty is primarily due to the uncertainty of the flight-path difference $d_2 - d_1$; the uncertainty given by MINUIT (including the "scale factor") is 0.00006 cm/ns.

If the pionic hydrogen atom $(\pi^- p)$ is at rest at the time t_0 of reaction (1), the relation between the mass difference D_π and the kinetic energy T_n of the neutron is

$$D_\pi = m_{\pi^-} - m_{\pi^0}$$
$$= m_{\pi^-} - [(M_{\pi p} - m_n)^2 - 2T_n M_{\pi p}]^{1/2}, \tag{5}$$

where m_{π^-}, m_{π^0}, m_n, and $M_{\pi p}$ are respectively the masses of the charged and the neutral pion, the neutron, and the $\pi^- p$ atom. $M_{\pi p}$ is related to the binding energy E_B of the $\pi^- p$ atom at t_0 through the equation $M_{\pi p} = m_{\pi^-} + m_p - E_B$. The uncertainties of m_{π^-}, m_n, and m_p, taken from Ref. 1, can be shown[9] to make negligible contributions to the uncertainty $\sigma(D_\pi)$.

In liquid hydrogen reaction (1) has been calculated[10] to occur predominantly from $\pi^- p$ atomic states with principal quantum numbers $n = 3$ or 4, while capture from the ground state, $n = 1$, has been measured[11] to occur in at most a few percent of all cases. The uncertainty of the $\pi^- p$ binding energy is thus also negligible[9] and the only relevant contribution to the uncertainty $\sigma(D_\pi)$ comes from the neutron velocity v_n.

If the $\pi^- p$ atom is not at rest at t_0, its velocity, v_0, will add to v_n. One can show[12] that if the v_0 are isotropically distributed and smaller than v_n, they will not

change the mean TOF of the neutrons but will cause a distance-dependent spread of the TOF distribution. This spread can be shown[12] to be related to the mean kinetic energy $\bar{T}_{\pi p}$ of the $\pi^- p$ atoms at t_0 through

$$\bar{T}_{\pi p} = \tfrac{3}{2} M_{\pi p} v_{n0}^4 \sigma_d^2. \tag{6}$$

Here v_{n0} is the neutron velocity for $T_{\pi p} = 0$, and $\sigma_d d$ the standard deviation of the neutron TOF peak due to the motion of the $\pi^- p$ atoms, where d is the length of the neutron flight path.

From our result for the neutron velocity (4) and Eq. (5) we calculate the mass difference D_π to be

$$D_\pi = m_{\pi^-} - m_{\pi^0} = 4.5930 \pm 0.0013 \text{ MeV}/c^2. \tag{7}$$

Our result for D_π differs from the previous world average[1] $D_\pi(\text{old}) = 4.6043 \pm 0.0037$ MeV/c^2, which was dominated by Refs. 7 and 13, by almost 3 standard deviations.

The result for the parameter σ_d^2 related to the motion of the $\pi^- p$ atom [cf. Eq. (6)] is

$$\sigma_d^2 = 0.054 \pm 0.040 \text{ (ns/m)}^2. \tag{8}$$

In Ref. 7 the standard deviation of the neutron velocity distribution is derived from the TOF spectra to be $(8.0 \pm 1.5) \times 10^6$ cm/s which corresponds to σ_d^2 (Ref. 7) $= 1.00 \pm 0.38$ (ns/m)^2. Again our result (8) differs strongly from the old result, which, if correct, would give a linewidth of 20 ns (FWHM) for the neutron TOF peak in Fig. 3.

Inserting Eq. (8) into Eq. (6) gives a mean kinetic energy $\bar{T}_{\pi p}$ of the $\pi^- p$ atoms at the time of reaction (1) of

$$\bar{T}_{\pi p} = 6.2 \pm 4.6 \text{ eV}. \tag{9}$$

The mean energy $\bar{T}_{\pi p}$ has been estimated[10] to be about 1 eV. Our result (9) is consistent with that estimate. In view of the large uncertainty of $\bar{T}_{\pi p}$ we prefer, however, to quote an upper limit derived from Eq. (9),

$$\bar{T}_{\pi p} < 12 \text{ eV (90\% C.L.)}. \tag{10}$$

[1]C. G. Wohl et al. (Particle Data Group), Rev. Mod. Phys. 56, S1 (1984).

[2]W. K. McFarlane et al., Phys. Rev. D 32, 547 (1985).

[3]K. Borer et al., unpublished.

[4]M. Gettner et al., Phys. Rev. Lett. 2, 471 (1959).

[5]R. P. Haddock et al., Phys. Rev. Lett. 3, 478 (1959).

[6]P. Hillman et al., Nuovo Cimento 14, 887 (1959).

[7]John B. Czirr, Phys. Rev. 130, 341 (1963).

[8]F. James and M. Roos, CERN 6600 Computer Program Library D507 (1967).

[9]J. F. Crawford et al., unpublished.

[10]M. Leon and H. A. Bethe, Phys. Rev. 127, 636 (1962).

[11]B. Budick et al., Phys. Lett. 34B, 539 (1971).

[12]R. Frosch, Schweizerisches Institut für Nuklearforschung Internal Report No. TM-37-21, 1985 (unpublished).

[13]I. M. Vasilevsky et al., Phys. Lett. 23, 281 (1966).